

Small- and Large-Scale Galactic Conformity in SDSS DR7

Victor F. Calderon^{1*}, Andreas A. Berlind¹, Manodeep Sinha^{1,2,3}

¹*Department of Physics and Astronomy, Vanderbilt University, Nashville, TN 37235, USA*

²*Centre for Astrophysics and Supercomputing, Swinburne University of Technology, Hawthorn, Victoria 3122, Australia*

³*ARC Centre of Excellence for All Sky Astrophysics in 3 Dimensions (ASTRO 3D)*

Accepted XXX. Received YYY; in original form ZZZ

ABSTRACT

Galactic conformity is the phenomenon whereby galaxy properties exhibit excess correlations across distance than that expected if these properties only depended on halo mass. We perform a comprehensive study of conformity at low redshift using a galaxy group catalogue from the SDSS DR7 spectroscopic sample. We study correlations both between central galaxies and their satellites (1-halo), and between central galaxies in separate haloes (2-halo). We use the quenched fractions and the marked correlation function (MCF), to probe for conformity in three galaxy properties, $(g-r)$ colour, specific star formation rate (sSFR), and morphology. We assess the statistical significance of conformity signals with a suite of mock galaxy catalogues that have no built-in conformity, but contain the same group-finding and mass assignment errors as the real data. In the case of 1-halo conformity, quenched fractions show strong signals at all group masses. However, these signals are equally strong in mock catalogues, indicating that the conformity signal is spurious and likely entirely caused by group-finding systematics, calling into question previous claims of 1-halo conformity detection. The MCF reveals a significant detection of radial segregation within massive groups, but no evidence of conformity. In the case of 2-halo conformity, quenched fractions show no significant evidence of conformity in colour or sSFR once compared with mock catalogues, but a clear signal using morphology. In contrast, the MCF reveals a small, yet highly significant signal for all three properties in low mass groups and scales of $0.8-4h^{-1}\text{Mpc}$, possibly representing the first robust detection of 2-halo conformity.

Key words: cosmology: observations — cosmology: large-scale structure of Universe — galaxies: groups — galaxies: clusters — methods: statistical

1 INTRODUCTION

Characterizing the relation between the properties of galaxies and their host dark matter (DM) haloes – referred to as the “galaxy-halo” connection – has emerged as a powerful tool to constrain theories of galaxy formation with statistical measurements in galaxy surveys. The phenomenon called “*galactic conformity*” is a subtle feature of this galaxy-halo connection, whereby galaxy properties are spatially correlated even *at fixed halo mass*. Specifically, several studies have claimed to detect a correlation between quenching properties of galaxies, such as morphology, gas content, star formation rate, neutral hydrogen content, and broadband colour, and those of neighbouring galaxies (Weinmann et al. 2006; Ann et al. 2008; Ross & Brunner 2009; Kauffmann et al. 2010; Prescott et al. 2011; Wang & White 2012; Kauffmann et al. 2013; Knobel et al. 2015; Hartley et al. 2015; Wang et al. 2015; Kawinwanichakij et al. 2016; Berti

et al. 2017; Zu & Mandelbaum 2018). This effect of “galactic conformity” exists over two distance regimes, both between central and satellite galaxies within the same halo, and between galaxies separated by several virial radii of their haloes. We refer to these regimes as “1-halo” and “2-halo” conformity, respectively (Hearin et al. 2015). 2-halo conformity is closely linked to “halo assembly bias” or “secondary bias” (e.g., Gao et al. 2005; Wechsler et al. 2006; Salcedo et al. 2017), whereby the clustering of haloes depends on secondary properties, like age, at fixed mass, and “galaxy assembly bias” (e.g., Croton et al. 2007), whereby galaxies inherit this clustering when their observed properties correlate with these secondary halo properties. Assembly bias provides a natural explanation for 2-halo conformity (Hearin et al. 2015, 2016).

Conformity detections are notoriously difficult to make because it is hard to be confident that measurements are truly being made at fixed halo mass and also to know whether a given galaxy pair lives in the same halo or not. At the present time, there are several detection claims of 1-

* E-mail: victor.calderon@vanderbilt.edu

halo conformity at both low and high redshifts. These studies have looked at correlations between galaxy properties of the central galaxies and their respective satellite galaxies. Some have used isolation criteria to distinguish between centrals and satellites, while others have used group galaxy catalogues to do this. However, the impact of systematic errors on these results has not been quantified. In the 2-halo regime, conformity has not yet been detected, as a couple recent works showed convincingly that past detections were entirely caused by selection biases. The current state of affairs for both 1-halo and 2-halo galactic conformity is still inconclusive and it is thus important to investigate this further.

The term “galactic conformity” was first coined by Weinmann et al. (2006, hereafter W06) after finding a correlation between the colours and star formation rates (SFR) of central and satellite galaxies in common Yang et al. (2005) galaxy groups of similar mass at low-redshifts, i.e. $z < 0.05$, in SDSS (York et al. 2000) DR2 (Abazajian et al. 2004). Specifically, W06 found that in galaxy groups of similar mass, quenched satellite galaxies occur more frequently around quenched central galaxies than around star-forming central galaxies. Controlling for halo mass is of critical importance in conformity studies because the SFRs of both centrals and satellites decrease with halo mass, which can naturally induce a conformity-like signal. W06 attempted to control for halo mass by adopting bins in total group luminosity.

Several subsequent studies also found correlations in SFR and other properties between central and satellite galaxies, using different methods for distinguishing between centrals and satellites and different ways of controlling for mass. Ann et al. (2008) used isolation criteria, rather than a group catalogue, to identify centrals and satellites in SDSS DR5 (Adelman-McCarthy et al. 2007). They found that early-type satellite galaxies tend to reside in the vicinity of early-type central galaxies, and argue that this conformity in morphology is likely due to hydrodynamic and radiative influence of central galaxies on satellite galaxies, in addition to tidal effects. They attempted to control for mass by restricting their analysis to central galaxies in a limited range of luminosity. Wang & White (2012) also used isolation criteria to study correlations between isolated bright primary galaxies in SDSS DR7 (Abazajian et al. 2009) and nearby secondary galaxies (i.e., satellites) in SDSS DR8 (Aihara et al. 2011). They found that the colour distribution of satellites is redder for red primaries than for blue primaries of the same stellar mass. This is a similar 1-halo conformity trend in colour as found by W06, except that Wang & White (2012) control for central galaxy stellar mass. In addition, Wang & White (2012) compared their results to the Guo et al. (2011) semi-analytic model (SAM). They found that the SAM predicted a similar conformity signal as the SDSS. However, when they re-analysed the SAM controlling for halo mass instead of central galaxy stellar mass, they found a substantially reduced signal. This implies that a large portion of their observed SDSS conformity signal could be due to halo mass differences between red and blue galaxies at fixed stellar mass. Phillips et al. (2014a,b) also used isolation criteria to study the SFR of $\sim 0.1L^*$ satellites around isolated $\sim L^*$ central galaxies in the local Universe using SDSS DR7. They found that satellites of quiescent primaries are more than twice as likely to be quenched than similar mass satel-

lites of star forming primaries. Unlike other studies, these authors control for the stellar mass of satellites, rather than centrals. This might seem risky since satellite galaxy stellar mass is not expected to correlate strongly with halo mass. However, the authors compare the velocity distributions of satellites around star forming and quiescent primaries and they conclude that the difference in halo mass between the two samples is not large enough to account for the conformity signal they observe. Finally, Knobel et al. (2015) used the Yang et al. (2012) group catalogue in SDSS DR7 to study the degree of central-satellite conformity, controlling for several combinations of properties, including total group stellar mass. They confirmed that satellites of quenched central galaxies are more likely to be quenched than those of active central galaxies.

Ross & Brunner (2009) found evidence of 1-halo conformity using a completely different approach. They used a Halo Occupation Distribution (HOD; Berlind & Weinberg 2002) model to fit the clustering of photometric samples in SDSS DR5. They found that they could only simultaneously match the clustering of all, early- and late-type galaxies with a model that segregates early- and late-type galaxies into separate haloes as much as possible. This is similar in spirit to the previous work of Zehavi et al. (2005) who modelled the cross-correlation function between red and blue galaxies in SDSS DR2, though that study concluded that red and blue galaxies are well mixed within their haloes. Zehavi et al. (2010) revisited this issue using SDSS DR7 and found significant evidence of colour segregation into different haloes, but the degree of segregation was much less than that found by Ross & Brunner (2009).

There have also been studies that have claimed a detection of 1-halo conformity at higher redshift. Hartley et al. (2015) used isolation criteria in the UKIDSS (Lawrence et al. 2007) Ultra Deep Survey DR8, to explore the redshift evolution of the correlation between the SFR of central galaxies and satellite galaxies at intermediate to high redshifts ($0.4 < z < 1.9$). They confirmed that passive satellites tend to be preferentially located around passive central galaxies, and showed that the trend persists to at least $z \sim 2$ without any significant evolution. Kawinwanichakij et al. (2016) carried out a similar analysis and identified central and satellite galaxies in the range of $0.3 < z < 2.5$ by combining imaging from three deep near-infrared-selected surveys ZFOURGE/CANDELS, UDS, and UltraVISTA (McCracken et al. 2012) and deriving accurate photometric redshifts. They found that, at similar central stellar mass, satellites of quiescent central galaxies are more likely to be quenched compared to satellites of star-forming central galaxies. This conformity signal is only significant at $0.6 < z < 1.6$, and becomes weaker at both lower and higher redshifts. Kawinwanichakij et al. (2016) argue that their detection is unlikely to arise from any difference in halo mass between star-forming and quiescent centrals. To check this they allowed for star-forming centrals to have a stellar mass of up to 0.2 dex higher than quiescent centrals and found that, though the conformity signal weakens, it does not vanish. Most recently, Berti et al. (2017) used isolation criteria in the spectroscopic PRIMUS Survey (Coil et al. 2011; Cool et al. 2013) to look for conformity at $0.2 < z < 1.0$. After matching the stellar mass and redshift distributions of star-forming and quenched centrals, Berti et al. (2017) claimed a 3σ detection of a $\sim 5\%$ excess of star-

forming neighbours around star-forming central galaxies on scales of 0-1 Mpc. This conformity signal is substantially weaker than the W06 signal observed in SDSS at $z \lesssim 0.05$. Berti et al. (2017) also reported on a 2-halo conformity detection, albeit with weaker statistical significance.

In the 2-halo regime, Kauffmann et al. (2013, hereafter K13) claimed a detection of conformity using a volume-limited sample of galaxies with redshifts $z < 0.03$ from the SDSS DR7. They adopted isolation criteria to identify central galaxies and studied the median specific SFR of neighbouring galaxies as a function of different properties of the centrals. K13 found that the SFR of neighbours correlates with that of centrals, even up to 4 Mpc, a distance that is well outside the virial radius of the primary galaxy's halo. This 2-halo conformity signal is present for low stellar mass galaxies, with massive galaxies only exhibiting a 1-halo conformity signal. The K13 result was intriguing and motivated a number of theoretical studies to explain it. However, a pair of recent studies have shown convincingly that the result in K13 is entirely due to selection bias. Tinker et al. (2018, hereafter T17) reproduced the result of K13 and then used a group finding algorithm and a mock catalogue to show that the majority of the 2-halo conformity signal comes from a subset of satellite galaxies that were mis-identified as primaries in the galaxy sample. After removing this small fraction of satellite galaxies, T17 detect no statistically significant 2-halo conformity in galaxy star formation rates. Sin et al. (2017, hereafter S17) carried out a similar analysis, and argued that the isolation criteria in K13 could potentially include low-mass central galaxies in the vicinity of massive systems, and that the large-scale conformity signal is likely a short-range effect coming from massive haloes. In addition to the misclassification of satellite galaxies as central galaxies in the isolation criteria, S17 argued that a weighting in favour of central galaxies in very high-density regions, and the use of medians to characterize the bimodal distribution of sSFR could potentially amplify the large-scale conformity signal seen in K13.

Zu & Mandelbaum (2018) came to a similar conclusion about the lack of 2-halo conformity by finding that conformity measurements in SDSS DR7 are consistent with predictions from the iHOD *halo-quenching* model (Zu & Mandelbaum 2015, 2016), in which galaxy colours depend *only* on halo mass. This suggests that all conformity signals are simply due to the combination of the environmental dependence of the halo mass function combined with the strong correlation between galaxy colours and halo mass. In other words, no galaxy assembly bias or other environmental quenching mechanisms are required to explain 2-halo conformity signals.

On the theoretical side, there have been several studies looking at both 1-halo and 2-halo conformity. Paranjape et al. (2015) called into question the conformity signal measured by K13 at a projected distance of $\lesssim 4$ Mpc by generating mock catalogues with varying levels of built-in galactic conformity, and comparing these to SDSS galaxies in the Yang et al. (2007) galaxy group catalogue. They argued against the K13 result being evidence of galaxy and halo assembly bias. Paranjape et al. (2015) also argued that only at very large separations, ($\gtrsim 8$ Mpc), does 2-halo conformity, driven by the assembly bias of small haloes, manifest distinctly. They suggest that the observed conformity at $\lesssim 4$

Mpc is simply due to central galaxies of similar stellar mass residing in haloes of different masses. Other papers have tried to explore the origin of galactic conformity. Hearin et al. (2016) studied the correlation between the mass accretion rates of nearby haloes as a potential physical origin for 2-halo galactic conformity. They found that pairs of host haloes have correlated assembly histories, despite being separated from each other by distances greater than thirty virial radii at the present day. They presented halo accretion conformity as a plausible mechanism driving 2-halo conformity in SFR. Moreover, they argued that galactic conformity is related to large-scale tidal fields, and predicted that 2-halo conformity should generically weaken at higher redshift and vanish to undetectable levels by $z \sim 1$. In this context, the 2-halo galactic conformity signal in Berti et al. (2017) is consistent with the Hearin et al. (2016) prediction and Berti et al. (2017) state that their detection of galactic conformity is thus likely indicative of assembly bias and arises from large-scale tidal fields. Additionally, Bray et al. (2016) investigated the role of assembly bias in producing galactic conformity in the Illustris (Vogelsberger et al. 2014) simulation, and argued to have found 2-halo conformity in the red fraction of galaxies. They found that, at fixed stellar mass, the red fraction of galaxies around redder neighbour galaxies is higher than it is around bluer galaxies and this effect persists out to distances of 10 Mpc. They concluded by saying that the predicted amplitude of the conformity signal depends on the projection effects, stacking techniques, and the criteria used for selecting central galaxies. Lacerna et al. (2018) used three semi-analytic models to study the correlations between sSFR of central galaxies and neighbour galaxies out to scales of several Mpc. They predicted a strong 1-halo galactic conformity signal when the selection of primary galaxies was based on an isolation criterion in real space, and claimed a significant 2-halo conformity signal as far as ~ 5 Mpc. However, the overall signal of galactic conformity decreased when satellites that had been misclassified as central galaxies were removed in the selection of primary galaxies. The authors concluded that the SAMs used in the analysis do not show galactic conformity for the 2-halo regime.

Galactic conformity remains a debated topic, and it is unclear if all previous detection claims are valid. The work of Campbell et al. (2015) exposed the dangers of using group catalogues to study 1-halo conformity. They showed that group finders do a good job at recovering galactic conformity, but they also tend to introduce weak conformity when none is present in the data. This calls into question previous claims, such as the one by W06. More recently, T17 and S17 challenged the measurement of 2-halo conformity made by K13 by showing that their isolation criteria were not sufficiently robust. These conflicting results open the door for improvements in the measurements of 1-halo and 2-halo conformity. In this paper we investigate both regimes using a galaxy group catalogue from the SDSS DR7. Our analysis contains three main improvements over previous works. First, we study three observed properties of galaxies: $(g-r)$ colour, sSFR, and Sérsic index. Second, we use a new statistic, the marked correlation function, $\mathcal{M}(r_p)$, in addition to the previously used quenched fractions. $\mathcal{M}(r_p)$ is ideally suited for conformity studies and is a more sensitive probe of weak conformity signals. Third, we use a suite of 100 mock galaxy catalogues to quantify the statistical sig-

nificance of our results. The mock catalogues do not have any built-in conformity, but they are affected by the same systematic errors as the SDSS data. By comparing our SDSS measurements to the distribution of mock measurements, we can quantify the probability that whatever signal we detect could have arisen from a model with no conformity.

This paper is organized as follows. In §2, we describe the observational and simulated data used in this work, as well as the main analysis methods. In §3, we present a detailed examination of galactic conformity, distinguishing between 1-halo (§3.1) and 2-halo (§3.2). We summarize our results and discuss their implications in §4. The Python codes and the catalogues used in this project will be made publicly available on Github¹ upon publication of this paper.

2 DATA AND METHODS

In this section, we present the datasets used throughout this analysis, and introduce the main statistical methods that we use to search for conformity signals. In §2.1 we briefly describe the SDSS galaxy sample that we use, along with the parameters that are included in this catalogue. In §2.2 we summarize how we identify galaxy groups and estimate their masses. In §2.3 we describe in detail the mock catalogues that we use throughout the paper. Finally, we describe the two main statistical methods for probing conformity in §2.4 and §2.5.

2.1 SDSS Galaxy Sample

For this analysis, we use data from the Sloan Digital Sky Survey. SDSS collected its data with a dedicated 2.5-meter telescope (Gunn et al. 2006), camera (Gunn et al. 1998), filters (Doi et al. 2010), and spectrograph (Smee et al. 2013). We construct our galaxy sample from the **large-scale structure** sample of the NYU Value-Added Galaxy Catalogue (NYU-VAGC; Blanton et al. 2005), based on the spectroscopic sample in Data Release 7 (SDSS DR7; Abazajian et al. 2009). The main spectroscopic galaxy sample is approximately complete down to an apparent r -band Petrosian magnitude limit of $m_r = -17.77$. However, we have cut our sample back to $m_r = -17.6$ so it is complete down to that magnitude limit across the sky. Galaxy absolute magnitudes are k -corrected (Blanton et al. 2003) to rest-frame magnitudes at redshift $z = 0.1$.

We construct a volume-limited galaxy sample that contains all galaxies brighter than $M_r = -19$, and we refer to this sample as Mr19-SDSS. The redshift limits of the sample are $z_{\min} = 0.02$ and $z_{\max} = 0.067$ and it contains 90,893 galaxies with a number density of $n_{\text{gal}} = 0.01503 h^3 \text{Mpc}^{-3}$. The sample includes the right ascension, declination, redshift, Sérsic index, and $(g-r)$ colour for each galaxy.

To each galaxy, we assign a star formation rate (SFR) using the MPA Value-Added Catalogue DR7². This catalogue includes, among many other parameters, stellar masses based on fits to the photometry using Kauffmann et al.

(2003) and Salim et al. (2007), and star formation rates based on Brinchmann et al. (2004). We cross-match the galaxies of the NYU-VAGC catalogue to those in the MPA-JHU catalogue using their MJD, plate ID, and fibre ID. A total of 5.85% of galaxies in the sample did not have corresponding values of SFR and we remove them from the sample. This leaves a sample of 85,578 galaxies. For each of these galaxies, we divide its SFR by its stellar mass to get a specific star formation rate sSFR.

sSFR and $(g-r)$ colour are highly correlated galaxy properties with the main difference coming from dust attenuation that moves some intrinsically star forming galaxies onto the red sequence. However, we have chosen to use both galaxy properties in this analysis in order to facilitate the comparison of our work to previous claims of conformity detection.

2.2 Group Finding Algorithm and Mass Assignment

We identify galaxy groups using the Berlind et al. (2006) group-finding algorithm. This is a Friends-of-Friends (FoF; Huchra & Geller 1982) algorithm that links galaxies recursively to other galaxies that are within a cylindrical linking volume. The projected and line-of-sight linking lengths are $b_{\perp} = 0.14$ and $b_{\parallel} = 0.75$ in units of the mean inter-galaxy separation. This choice of linking lengths was optimized by Berlind et al. (2006) to identify galaxy systems that live within the same dark matter halo. In each group, we define the most luminous galaxy (in the r -band) to be the ‘central’ galaxy. The rest of the galaxies are defined as ‘satellite’ galaxies.

We estimate the total masses of the groups via *abundance matching*, using total group luminosity as a proxy for mass. Specifically, we assume that the total group r -band luminosity L_{group} increases monotonically with halo mass M_h , and we assign masses to groups by matching the cumulative space densities of groups and haloes:

$$n_{\text{group}}(> L_{\text{group}}) = n_{\text{halo}}(> M_h). \quad (1)$$

To calculate the space densities of haloes, we adopt the Warren et al. (2006) halo mass function assuming a cosmological model with $\Omega_m = 1 - \Omega_{\Lambda} = 0.25$, $\Omega_b = 0.04$, $h \equiv H_0 / (100 \text{ km s}^{-1} \text{ Mpc}^{-1}) = 0.7$, $\sigma_8 = 0.8$, and $n_s = 1.0$. We refer to these abundance matched masses as *group masses*, M_{group} .

2.3 Mock Galaxy Catalogues

To quantify the statistical significance of any conformity signal that we measure using our SDSS groups, it is necessary to compare to a null model (i.e., no intrinsic conformity) that incorporates the same systematic errors as our measurements and also includes robust error distributions. For this purpose, we construct a suite of 100 realistic mock catalogues that are based on the *Large Suite of Dark Matter Simulations* (LasDamas) project³ (McBride et al. 2009).

We start with a set of 50 cosmological N-body simulations that trace the evolution of dark matter in the Universe and have sufficient volume and mass resolution to properly

¹ https://github.com/vcalderon2009/SDSS_Conformity_Analysis

² <http://www.mpa-garching.mpg.de/SDSS/DR7>

³ <http://lss.phy.vanderbilt.edu/lasdamas/>

model the Mr19-SDSS sample. These simulations assumed the same cosmological model described at the end of §2.2. Dark matter haloes were identified with a FoF algorithm (Davis et al. 1985) using a linking length of 0.2 times the mean inter-particle separation. We used an HOD model to populate the DM haloes with central and satellite galaxies, whose numbers as a function of halo mass were chosen to reproduce the number density, n_{gal} , and the projected 2-point correlation function, $w_p(r_p)$, of the Mr19-SDSS sample. Each central galaxy was placed at the minimum of the halo gravitational potential and was assigned the mean velocity of the halo. Satellite galaxies were assigned the positions and velocities of randomly chosen dark matter particles within the halo. Within each simulation box, we applied redshift space distortions and then we carved out two independent volumes that precisely mimic the geometry of our Mr19-SDSS sample. This procedure yields 100 independent mock catalogues from the 50 simulation boxes.

To assign a luminosity to each mock galaxy, we adopt the formalism of the *conditional luminosity function* (CLF; Yang et al. 2003; Van Den Bosch et al. 2003) that specifies functional forms for the luminosity distributions of central and satellite galaxies as a function of halo mass. Specifically, we use the Cacciato et al. (2009) version of the CLF, but modified slightly to match our adopted cosmological model (Van den Bosch, private communication). We then abundance match the luminosities obtained from the CLF to the r -band absolute magnitudes in Mr19-SDSS. As a result, our mock catalogues have the same exact luminosity function as the SDSS data.

We assign specific star formation rates, $(g-r)$ colours and Sérsic indices to mock galaxies by first adopting the formalism presented in Zu & Mandelbaum (2016, hereafter Z16), and then sampling from the original distributions of sSFR, $(g-r)$ colour and Sérsic indices of Mr19-SDSS. Specifically, we adopt the ‘halo’ quenching model from Z16, which assumes that halo mass is the sole driver of galaxy quenching. According to that model, the red/quenched fraction of central and satellite galaxies is given by

$$f_{\text{cen}}^{\text{red}}(M_h) = 1 - \exp\left[-(M_h/M_h^{\text{qc}})^{\mu^c}\right] \quad (2)$$

and

$$f_{\text{sat}}^{\text{red}}(M_h) = 1 - \exp\left[-(M_h/M_h^{\text{qs}})^{\mu^s}\right], \quad (3)$$

where M_h^{qc} , M_h^{qs} , μ^c , and μ^s are parameters of the model that Z16 fit to the observed clustering and galaxy-galaxy lensing measurements of red and blue galaxies in the SDSS. We assign each of our mock galaxies a probability of being quenched from equations (2) and (3) and we randomly designate it as ‘active’ or ‘passive’ consistent with that probability (e.g., if $f_{\text{sat}}^{\text{red}} = 0.8$ for a particular mock satellite galaxy, we give it an 80% chance of being labelled ‘passive’). To assign realistic values of sSFR, $(g-r)$ colour, and Sérsic index to mock galaxies, we divide the observed distributions of these properties of Mr19-SDSS into ‘active’ and ‘passive’ distributions by making cuts at $\log_{10} \text{sSFR} = -11$, $(g-r)_{\text{cut}} = 0.75$ and $n_{\text{cut}} = 3$ for sSFR, $(g-r)$ colour, and Sérsic index, respectively. For example, to assign sSFR values to mock galaxies, we do the following. For each mock galaxy, we randomly draw a sSFR value from the active or passive distribution, depending on the designation that the mock galaxy has received. Moreover, we do this in a way that preserves the joint

sSFR-luminosity distribution. For example, if a mock galaxy has been labelled ‘active’, we randomly select a real active galaxy from Mr19-SDSS that has a similar luminosity as the mock galaxy, and we assign its sSFR to the mock galaxy. As a result of this procedure, the final joint sSFR-luminosity distribution of mock galaxies closely resembles the one for Mr19-SDSS. However, the model contains *no intrinsic* 1-halo or 2-halo conformity because the galaxy sSFR values *only* depend on halo mass. We apply this same procedure to assign $(g-r)$ colours and Sérsic indices to each mock galaxy in order to preserve the joint distributions of these galaxy properties with luminosity as seen the Mr19-SDSS sample.

After constructing our 100 mock catalogues, we run the group-finding algorithm on each one to produce a corresponding group catalogue. We then label each mock galaxy as ‘central’ or ‘satellite’ and estimate total group masses by following the same methodology as in §2.2. The end result is a set of mock catalogues that do not have built-in galactic conformity in sSFR, $(g-r)$ colour, or Sérsic index, but suffer from the same kinds of systematics as the SDSS data, i.e. group-finding errors that lead to central-satellite misclassification and errors in the estimated group masses.

2.4 Quenched Fraction Difference Δf_q

Previous studies of conformity have mostly focused on measuring the fractions of quenched neighbour galaxies around active and passive primary galaxies, either as a function of group mass or as a function of distance (e.g., W06, K13). Following these studies, we also consider quenched fractions of neighbour galaxies, focusing on the *difference* between the fraction for passive primaries and that for active primaries. Moreover, we use three different galaxy properties to search for conformity: $(g-r)$ colour, sSFR, and Sérsic index. The cuts we use to designate galaxies as red, passive or early type are $(g-r) > 0.75$, $\log \text{sSFR} < -11$, and $n > 3$, respectively. These are the same cuts we discuss in §2.3.

To explain this better, let us consider the specific case of probing 1-halo conformity in galaxy colour. We measure the fraction of red satellite galaxies around red centrals, $P(\text{sat} = \text{red} \mid \text{cen} = \text{red})$, and the fraction of red satellite galaxies around blue centrals, $P(\text{sat} = \text{red} \mid \text{cen} = \text{blue})$. We then determine the *difference* between these two fractions, which we refer to as Δf_{red} . A conformity signal is then the case of $|\Delta f_{\text{red}}| > 0$. We define similar quantities using sSFR and morphology. The three quenched fraction differences that we measure are thus

$$\Delta f_{\text{red}} = P(\text{sat} = \text{red} \mid \text{cen} = \text{red}) \quad (4)$$

$$- P(\text{sat} = \text{red} \mid \text{cen} = \text{blue})$$

$$\Delta f_{\text{passive}} = P(\text{sat} = \text{passive} \mid \text{cen} = \text{passive}) \quad (5)$$

$$- P(\text{sat} = \text{passive} \mid \text{cen} = \text{active})$$

$$\Delta f_{\text{early}} = P(\text{sat} = \text{early} \mid \text{cen} = \text{early}) \quad (6)$$

$$- P(\text{sat} = \text{early} \mid \text{cen} = \text{late})$$

Finally, as a way to control for halo mass, we measure these fractions in bins of M_{group} . In the mock catalogues, we follow the same procedure to calculate Δf_{red} , $\Delta f_{\text{passive}}$ and Δf_{early} . For convenience, we refer to all three of these quantities as “quenched” fraction differences, Δf_q , recognizing that Sér-

sic index is a measure of galaxy morphology and not star formation activity.

In the case of 2-halo conformity, we use the same formalism of equations (4)–(6), with the difference that we only consider pairs of central galaxies with line-of-sight separations of $\pi_{\text{max}} < 20 h^{-1} \text{Mpc}$ and we calculate the fractions in bins of projected separation within each M_{group} bin. For each central-central galaxy, we designate one to be the primary and the other to be the secondary and we calculate the difference between the quenched fractions of secondary galaxies that are associated with quenched primaries and those that are associated with active primaries. Each galaxy pair contributes twice to the calculation of Δf_q because both galaxies get a turn at being considered the primary galaxy. For example, suppose there is a pair of galaxies, one red and one blue, that are both centrals in groups of similar mass. When the blue galaxy is the primary, the pair will contribute positively to the fraction $P(\text{secondary} = \text{red} \mid \text{primary} = \text{blue})$. On the other hand, when the red galaxy is the primary, the pair will contribute negatively to the fraction $P(\text{secondary} = \text{red} \mid \text{primary} = \text{red})$. Therefore, red-red and blue-blue pairs act to increase Δf_{red} , while red-blue pairs do the opposite. Δf_{red} essentially measures the excess number of similar pairs (i.e., red-red or blue-blue) over what one would expect if the population of red and blue galaxies were randomly mixed. The value of Δf_q ranges from +1 where all pairs are similar, to -1 where pairs are as different as possible.

2.5 Marked Correlation Function $\mathcal{M}(r_p)$

Galactic conformity is essentially a correlation between the properties of galaxies across distance. In the case of 1-halo conformity, we care about the correlation between properties of central galaxies and satellites within the same halo. In the case of 2-halo conformity, we look for a correlation between properties of central galaxies in separate haloes. The “*marked correlation function*” is an ideal tool for quantifying correlations across scale and it has been used successfully to probe the environmental dependence of galaxy properties (Beisbart & Kerscher 2000; Sheth et al. 2005; Skibba et al. 2006; Martinez et al. 2010).

The marked statistic $\mathcal{M}(r_p)$ provides a measure of the clustering of galaxy properties, or “marks”. In this paper, we analyse the marked statistics for $(g-r)$ colour, specific star formation rate (sSFR), and Sérsic index n in bins of group mass M_{group} . We adopt the formalism presented in Sheth et al. (2005) and Skibba et al. (2006) for defining $\mathcal{M}(r_p)$

$$\mathcal{M}(r_p) = \frac{1 + W(r_p)}{1 + \xi(r_p)} \equiv \frac{WW}{DD} \quad (7)$$

where $\xi(r_p)$ is the usual two-point correlation function with pairs summed in bins of projected separation r_p , and $W(r_p)$ is the same except that galaxy pairs are weighted by the product of their marks. The estimator used in equation (7) can also be written as WW/DD , where DD is the raw number of galaxy pairs separated by r_p and WW is the weighted number of pairs. Defining the statistic as a ratio in this way is advantageous because, unlike the correlation function, it can be estimated without explicitly constructing a random catalogue, but, like the correlation function, it accounts for

edge effects so one does not need to worry about the geometry of the survey (Sheth et al. 2005).

The marked statistic is essentially a measurement of the correlation coefficient between the marks of galaxies, as a function of projected separation. Though it is similar in spirit and goal to the quenched fraction difference statistic described in the previous section, the marked correlation function contains more information because it uses the full values of galaxy properties (e.g., colour) instead of just a binary classification (e.g., red or blue). There is thus reason to hope that $\mathcal{M}(r_p)$ is a more sensitive probe of galactic conformity than the usual quenched fractions.

3 GALACTIC CONFORMITY RESULTS

In this section, we present the results of the galactic conformity analysis of SDSS DR7. In §3.1, we investigate 1-halo conformity by looking at both quenched fraction differences, Δf_q , as a function of group mass (§3.1.1), and the mark correlation function, $\mathcal{M}(r_p)$, as a function of projected separation (§3.1.2). In §3.2, we investigate 2-halo conformity, also using Δf_q (§3.2.1) and $\mathcal{M}(r_p)$ (§3.2.2).

3.1 1-halo Conformity

3.1.1 Quenched Fractions and 1-halo Conformity

We first study 1-halo conformity using the quenched fraction difference statistic defined in §2.4 as a function of group mass. This is very similar to the original method that W06 used to detect 1-halo conformity. Specifically, we create six M_{group} bins of width 0.4 dex in the range $\log M_{\text{group}}$: 11.6–14.0. Within each bin of group mass, we make a list of all satellite galaxies that are in groups with a red central and a second list of all satellites in groups with a blue central. We then calculate the red fraction of satellites in each list and take the difference Δf_{red} . We repeat this process using sSFR and Sérsic index to calculate $\Delta f_{\text{passive}}$ and Δf_{early} . When using these quenched fraction differences, a conformity signal corresponds to values that are not zero, i.e., $|\Delta f_q| > 0$.

To determine the statistical significance of any conformity signal, we use a random shuffling method to eliminate any intrinsic conformity or correlation in the sample at the group level. Specifically, we shuffle the properties (colour, sSFR, Sérsic index) of all central and satellite galaxies within each group mass bin. Each central galaxy swaps properties with a randomly selected central galaxy from a different group of similar mass, and each satellite swaps properties with a randomly selected satellite from a group of similar mass. This procedure preserves the distributions of central and satellite properties as a function of group mass, but it explicitly erases any correlation between the properties of centrals and their satellites within any single group. The shuffling thus completely erases any 1-halo conformity signal that may exist in the data. We repeat this shuffling process a total of 1000 times (using different random seeds) and we re-measure the quenched fraction differences each time. The resulting distribution of $\Delta f_{q, \text{shuffle}}$ values thus allows us to quantify the probability that any measured conformity signal could be a statistical fluke. We find that the distribution of shuffle values is consistent with being Gaussian and so we

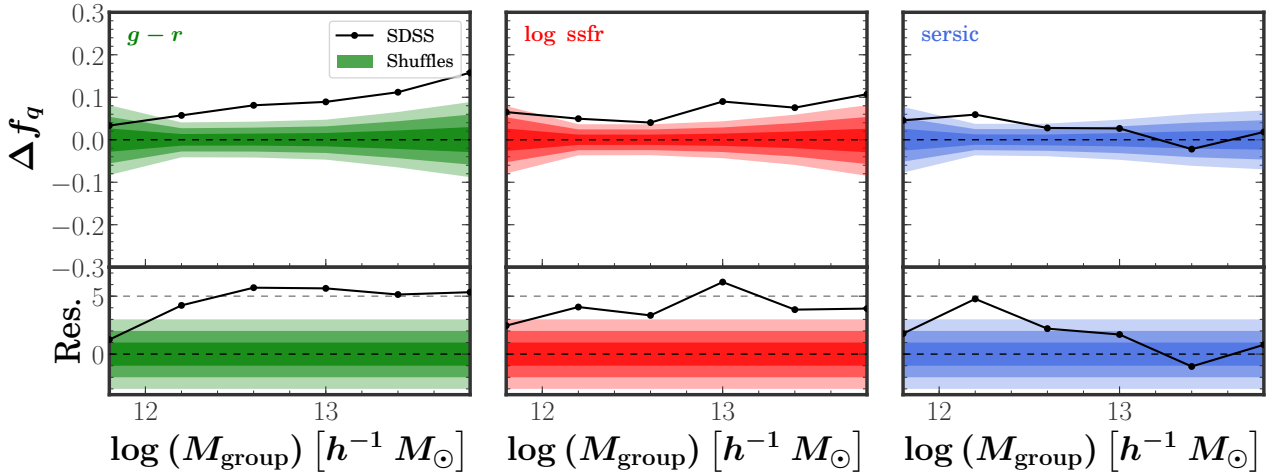


Figure 1. Difference of fractions, Δf , of red (left), passive (centre), and early-type (right) satellites as function of estimated group mass, M_{group} , where the difference is measured between groups with red and blue, passive and active, early-type and late-type central galaxies, as measured in the Mr19-SDSS sample. *Top panels:* The solid black lines correspond to the Δf of each galaxy property. The shaded contours show the 1σ , 2σ , and 3σ ranges of Δf calculated from many realizations in which the values of the galaxy properties are randomly shuffled, thus erasing any trace of 1-halo galactic conformity. *Bottom panels:* Normalised residuals of Δf of each galaxy property with respect to the shuffled realizations. The solid black lines show the difference between Δf and the mean of the shuffles, divided by the standard deviation of Δf for the shuffles. The shaded contours show the 1σ , 2σ , and 3σ ranges of the shuffled scenario in this normalised space.

use the standard deviation of the shuffled values to calculate the 1σ , 2σ , and 3σ ranges of the distribution of $\Delta f_{q,\text{shuffle}}$. We adopt the 3σ level as our detection threshold.

For each measurement of Δf_q on the un-shuffled data, we calculate the residual with respect to the shuffled data as

$$\text{Res} = \frac{\Delta f_q - \overline{\Delta f_{q,\text{shuffle}}}}{\sigma_{q,\text{shuffle}}} \quad (8)$$

where $\overline{\Delta f_{q,\text{shuffle}}}$ is the mean of the 1000 shuffles and $\sigma_{q,\text{shuffle}}$ is their standard deviation.

Figure 1 presents our main results of probing 1-halo conformity using quenched fraction differences. The black lines in the top three panels show the Δf_q for $(g-r)$ colour, sSFR, and Sérsic index, as measured in the Mr19-SDSS sample. The shaded contours show the 1σ , 2σ , and 3σ ranges of $\Delta f_{\text{shuffle}}$ for the *shuffle* cases of each galaxy property. The bottom panels show the residuals of each galaxy property with respect to the shuffles, as defined in equation (8). Figure 1 shows prominent conformity signals in the quenched fraction differences for $(g-r)$ colour and sSFR at large group masses, while for morphology the signal only appears at low group mass. Specifically, the conformity signal in colour rises with mass from $\Delta f_{\text{red}}=0.06$ to 0.14 and is at the $4-6\sigma$ level of statistical significance for masses above $10^{12} h^{-1} M_{\odot}$. In the case of sSFR, the signal is lower, rising from $\Delta f_{\text{passive}}=0.05$ to 0.1 and is at the $3-4\sigma$ level, except for a 6σ peak at $\sim 10^{13} h^{-1} M_{\odot}$. Finally, in the case of Sérsic index, the signal is only significant for groups of mass $\sim 10^{12.2} h^{-1} M_{\odot}$, where $\Delta f_{\text{early}}=0.07$ and has a statistical significance of $5-6\sigma$. These results are in agreement with the results shown in W06, who also find a significant difference in the red fraction at high masses and a slightly weaker signal when using sSFR.

We have found statistically significant correlations between the properties of central and satellite galaxies within

groups in Mr19-SDSS by comparing to the distribution of shuffled measurements, where any correlations between the properties of centrals and satellites have been erased. However, this does not mean that we have detected 1-halo galactic conformity, which is a correlation at fixed *halo* mass. Grouping errors that cause misidentification of centrals and satellites as well as errors in the estimated group mass M_{group} could be responsible for inducing a conformity-like signal (Campbell et al. 2015). To test this, we need to compare our measurements to mock catalogues that contain no built-in conformity, but are analysed in the same way as the SDSS data.

We apply the same procedure described above to the set of mock catalogues described in §2.3. The goal is to determine if the signal revealed in Figure 1 remains statistically significant when compared to the distribution of $\Delta f_{q,\text{mock}}$ measurements from the 100 mock catalogues with no conformity built-in. We find that the distribution of 100 values of $\Delta f_{q,\text{mock}}$ is approximately Gaussian and so we use their standard deviation to estimate the 1σ , 2σ , and 3σ ranges of the distribution. As we did previously for the shuffles, for each measurement of Δf_q on the SDSS data, we calculate the residual with respect to the mocks as

$$\text{Res} = \frac{\Delta f_q - \overline{\Delta f_{q,\text{mock}}}}{\sigma_{q,\text{mock}}} \quad (9)$$

where $\overline{\Delta f_{q,\text{mock}}}$ is the mean of the 100 mocks and $\sigma_{q,\text{mock}}$ is their standard deviation.

Figure 2 is analogous to Figure 1, except that the shaded contours now show the distribution of mocks rather than shuffles. The black lines in the top panels show the Δf_q for each galaxy property as measured in the Mr19-SDSS sample and are thus identical to the black lines in the three top panels of Figure 1. The shaded contours show the 1σ , 2σ , and 3σ ranges of $\Delta f_{q,\text{mock}}$ values of the mock catalogues. The

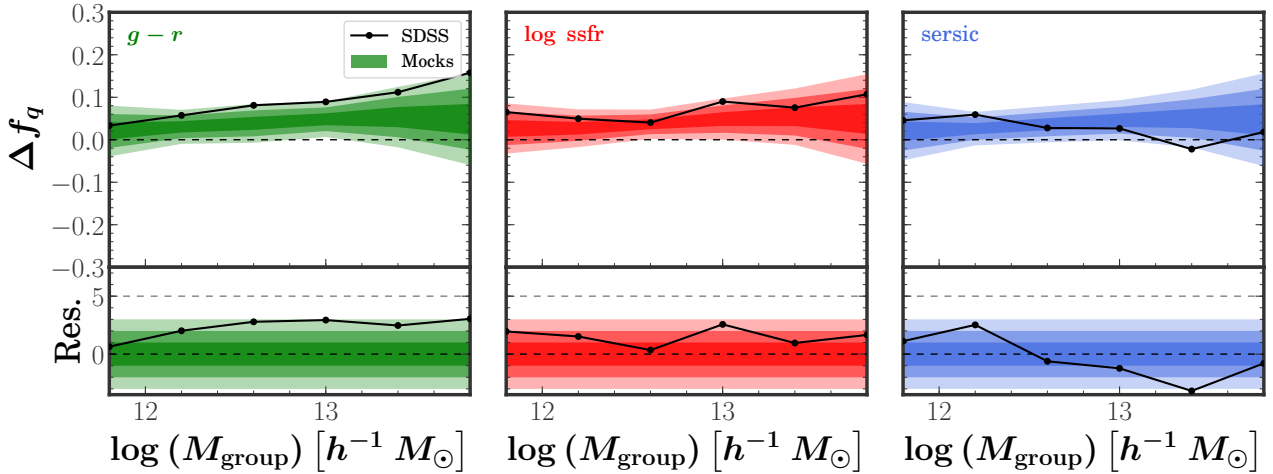


Figure 2. Similar to Figure 1, except that the Δf_q of Mr19-SDSS are compared to the distributions of measurements from mock catalogues rather than randomly shuffled data. *Top panels:* The solid black lines correspond to the Δf_q in Mr19-SDSS. The shaded contours show the 1σ, 2σ, and 3σ ranges of Δf_q calculated from 100 mock catalogues with no built-in conformity. *Bottom panel:* Normalised residuals of Δf_q with respect to the mock catalogues. The solid black lines show the difference between Δf_q for Mr19-SDSS and the mean of the mocks, divided by the standard deviation of the mocks. The shaded contours show the 1σ, 2σ, and 3σ ranges of the mocks in this normalised space.

bottom panels show the residuals with respect to the mocks, as defined in equation (9). The prominent conformity signals that we found previously disappear when compared against the mock catalogues. This is because the whole shaded bands are no longer centred at $\Delta f_q = 0$, but have shifted up significantly. In other words, the mock catalogues with no built-in conformity have an average quenched fraction difference of 0.02 to 0.05 for the three galaxy properties, depending on group mass. These *spurious* conformity signals must be due to grouping errors – either in misidentification of centrals and satellites, or in estimation of M_{group} . We have examined the contributions to the induced signal from both of these factors by constructing versions of our mock catalogues that do not contain these errors. We find that most of the induced signal comes from errors in assigning M_{group} , consistent with Campbell et al. (2015).

Figure 2 shows that the statistical significance of the 1-halo conformity signal in the quenched fractions of the Mr19-SDSS sample drops from 5–6σ when using the shuffles to 2.5–3σ when using the mocks. Consequently, we can no longer claim a significant detection of 1-halo galactic conformity. This result illustrates the importance of using mock catalogues to compute the null model (i.e., no conformity case) in any conformity analysis. Moreover, it is necessary to use a large suite of mock catalogues to properly specify the distribution of the null model. A few of our 100 mock catalogues do not display spurious conformity signals and so if we had only used one mock that happened to lack any conformity signals, we would have come to the wrong conclusion about the significance of our conformity detection. Our result calls into question previous claims of 1-halo conformity detections, especially from papers that used similar group-based methods as ours, including the original detection by W06.

3.1.2 $\mathcal{M}(r_p)$ for 1-halo Conformity

We now move to the second statistic that we are using to probe galactic conformity, the “marked correlation function”, $\mathcal{M}(r_p)$. Since the $\mathcal{M}(r_p)$ can be more sensitive than binary statistics, and can potentially uncover the scale dependence of any correlations (see discussion in §2.5), the $\mathcal{M}(r_p)$ is well-suited to exploring the correlations between central and satellite galaxies.

We evaluate $\mathcal{M}(r_p)$ for the three galaxy properties, i.e. $(g-r)$ colour, sSFR, and Sérsic index, in different bins of M_{group} . Each galaxy pair is comprised of a central galaxy and a satellite galaxy of the same galaxy group, and the projected distance, r_p , is the distance between the two member galaxies. We then take the product of the ‘marks’ of the two galaxies and average this over all pairs in bins of r_p . The mark for each galaxy is just the value of its property (e.g., colour) normalised by the mean value over the whole population of similar galaxies. We do this in two ways. First, we normalise using the mean of all central or satellite galaxies in the same bin of M_{group} . For example, the colour of each central (satellite) galaxy is divided by the mean colour of all central (satellite) galaxies that live in similar mass groups. $\mathcal{M}(r_p)$ then measures the correlation coefficient between the normalised colours of central and satellite galaxies. Since this measurement is done in r_p bins, it is sensitive to radial gradients in the properties of satellite galaxies within groups, typically referred to as *segregation*. For example, if groups contain colour segregation in the sense that satellite galaxies in the central regions of groups tend to be redder than satellite galaxies in the outskirts of groups, then $\mathcal{M}(r_p)$ will be larger than unity in bins of small r_p and less than unity in bins of large r_p . Such a radial segregation effect will masquerade as a 1-halo conformity signal. To account for this, we do a second normalization where the properties of satellite galaxies are normalised by the mean values of all satellites that live in the same bin of both M_{group} and

r_p . Measured in this way, $\mathcal{M}(r_p)$ is not sensitive to radial segregation and so values different from unity are direct indications of conformity.

To assess the statistical significance of a conformity signal while at the same time avoiding any biases due to grouping errors, we now only compare the results of the $\mathcal{M}(r_p)$ of Mr19-SDSS to those of the mock catalogues and not to those from the shuffling technique. By making this type of comparison, we avoid systematic errors that might masquerade as conformity signals. For example, it may be the case that galaxies that live in the outskirts of large groups are more likely to have been mis-assigned to their group than galaxies in the central regions of groups. These “satellites” may actually be centrals in much smaller neighbouring haloes that were incorrectly merged into the large groups. Since these low-mass centrals are likely to be bluer in colour than actual satellites of the large group, this error will masquerade as a radial colour gradient within groups. Such an effect may represent itself as an anti-correlation at large 1-halo scales. This type of systematic error will be present in the mocks as well and so we can account for the role of grouping errors by comparing our measurements to mock catalogues that contain no built-in conformity or segregation, but are analyzed in the same way as the SDSS data

Like we did for the quenched fraction differences in §3.1.1, we analyse the 100 mock catalogues in the same way as we analyse the Mr19-SDSS data. Specifically, we compute $\mathcal{M}(r_p)$ of each galaxy property, i.e. sSFR, $(g-r)$ colour, and Sérsic index, on the mocks after first normalizing each galaxy property the two different ways (in bins of M_{group} and in bins for both M_{group} and r_p). We use the standard deviation of $\mathcal{M}(r_p)$ values to estimate the 1σ , 2σ , and 3σ ranges of the distributions for each galaxy property. We then determine the statistical significance of the result by calculating the residuals of the SDSS measurements with respect to mocks as

$$\text{Res} = \frac{\mathcal{M}(r_p) - \overline{\mathcal{M}(r_p)_{\text{mock}}}}{\sigma_{\text{mock}}}. \quad (10)$$

This is similar to the residuals in equation (9).

Figure 3 shows $\mathcal{M}(r_p)$ of $(g-r)$ colour (left), sSFR (centre), and Sérsic index (right), as a function of projected distance, r_p , with each row corresponding to a bin of M_{group} . In this figure, we only show bins with $M_{\text{group}} > 10^{12.4} h^{-1} M_{\odot}$ since these exhibited the largest signals in the quenched fraction difference statistic for colour and sSFR, as shown in Figure 1. In the top part of each panel, the black, solid line corresponds to the $\mathcal{M}(r_p)$ of SDSS galaxies, when properties are normalised within bins of r_p in order to remove the effects of radial segregation. For comparison, the grey dashed line corresponds to the case when the segregation effect is included, i.e., the contributions for the $\mathcal{M}(r_p)$ results are coming from both galactic conformity and the segregation effect. The shaded regions correspond to the 1σ , 2σ , and 3σ ranges of the distributions of $\mathcal{M}(r_p)$ values for mock catalogues. However, these results are analysed by normalizing properties within bins of r_p , so only the black, solid lines can be compared to the shaded regions. We do not show the results that correspond to the grey, dashed lines. The bottom part of each panel shows the residuals of each $\mathcal{M}(r_p)$ with respect to the mock catalogues, as defined in equation (10). In

this case, the black solid lines and grey dashed lines are each computed using their corresponding set of mock results.

In Figure 3 the shaded regions for $(g-r)$ colour, sSFR, and Sérsic index are not centred at $\mathcal{M}(r_p) = 1$, indicating the effect of group errors. The strength of both radial segregation and conformity signals in the SDSS are weak when compared to mock catalogues containing neither effect. First we examine the case where we normalise galaxy properties by their mean values in bins of M_{group} , making $\mathcal{M}(r_p)$ sensitive to both conformity and segregation (dashed grey lines). We do detect significant radial segregation (dashed grey lines) for colour and sSFR at scales smaller than $0.2 h^{-1} \text{Mpc}$ in the case of massive groups, in the sense that satellite galaxies close to the centres of their groups tend to be more quenched (and thus more similar to their central galaxies) than satellite galaxies farther out. We do not find such correlations for the Sérsic index at those scales. Next we examine the case where radial segregation is removed (solid black lines). The 1-halo conformity signal hovers near the 3σ level for a wide range of small scales for colour and sSFR. However, the signal is not strong enough for us to claim a conformity detection. In summary, neither the quenched fractions nor the marked correlation function reveal any statistically significant 1-halo conformity signal after controlling for group errors for the cases of $(g-r)$ colour, sSFR, and Sérsic index.

3.2 2-halo Conformity

We next study 2-halo conformity, which is the correlation of properties for galaxies that live in separate haloes. As we discussed in §1, a detection of 2-halo conformity in sSFR was claimed by K13 for low-mass central galaxies out to scales of 4 Mpc. This claim has been challenged by T17 and S17 who reproduced the result of K13 and showed that the conformity signal is mainly driven by contamination in the isolation criterion to select the sample of central galaxies. After removing a small fraction of satellite galaxies that were misclassified as centrals from the primary sample, only a weak conformity signal remains out to projected distances of 2 Mpc.

3.2.1 Quenched fractions for 2-halo Conformity

We first analyse 2-halo conformity using the quenched fraction difference statistic, which is similar to what was used by some of these previous works. We use a sample composed of only central galaxies as classified by our group-finder, which are the most luminous galaxies in the r -band within their respective groups. Then, using the same group mass bins as before, we compute the quenched fraction difference statistic, as described in §2.4, in bins of projected separation r_p and only counting galaxy pairs within a line-of-sight separation of $\pi_{\text{max}} = 20 h^{-1} \text{Mpc}$. For example, to calculate Δf_{red} for the smallest group mass bin we consider, we first list all the central galaxies in groups with $\log M_{\text{group}}: 11.6\text{--}12.0$, then find all pairs of these galaxies that have line-of-sight separations less than π_{max} , and place them in logarithmic bins of r_p . Each radial bin now contains a set of central-central galaxy pairs where one of the galaxies is designated as “primary” and the other as “secondary” (each pair is counted twice so that both galaxies have a turn at being primary). We then

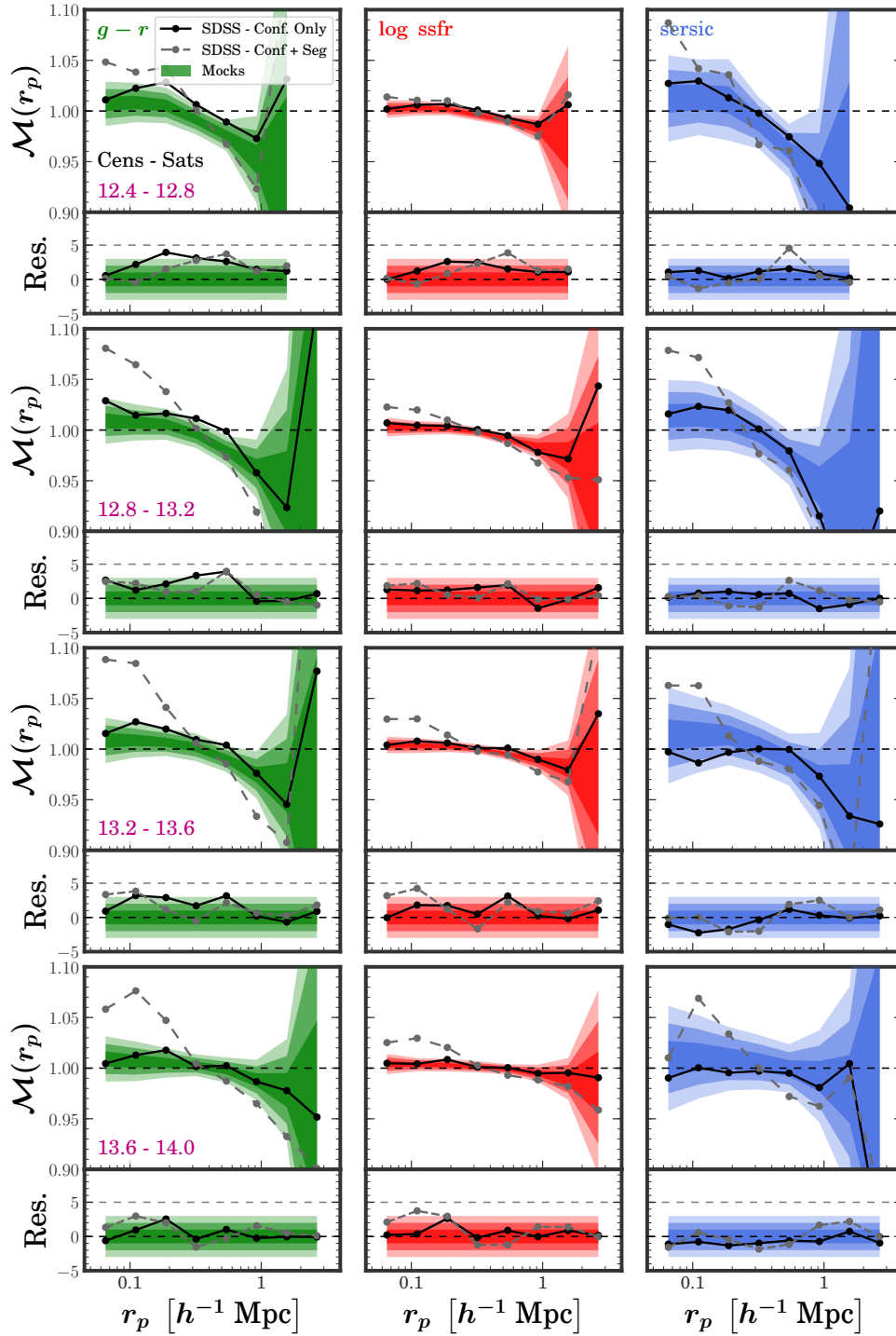


Figure 3. Marked correlation function, $\mathcal{M}(r_p)$, of $(g-r)$ colour (left), sSFR (centre), and Sérsic index (right), as a function of projected distance r_p for central-satellite galaxy pairs within the same galaxy groups in Mr19-SDSS and mock catalogues. Each row corresponds to a bin of group mass, M_{group} , as listed in the left panels. *Top panels:* The solid black lines correspond to the case where the marks have been normalised to remove the effects of radial segregation, while the dashed grey lines include segregation. The shaded contours show the 1σ , 2σ , and 3σ ranges of $\mathcal{M}(r_p)$ calculated from 100 mock catalogues with no built-in conformity or radial segregation. These mock results can only be compared to the solid black lines. We do not show the mock results that correspond to the dashed grey lines. *Bottom panels:* Normalised residuals of $\mathcal{M}(r_p)$ with respect to the mock catalogues. The lines show the difference between $\mathcal{M}(r_p)$ of the SDSS and the mean of the mocks, divided by the standard deviation of $\mathcal{M}(r_p)$ for the mocks. The solid black and dashed grey lines correspond to the cases where effects of radial segregation are removed and included, respectively. The shaded contours show the 1σ , 2σ , and 3σ ranges of the mocks in this normalised space.

make one list of pairs where the primary is red and another where it is blue. For each list we then calculate the fraction of pairs where the secondary is red (i.e., the “quenched fraction”) and we take the difference between these two fractions. We repeat this procedure for all group mass bins and for sSFR and Sérsic index. As before, we assess the statistical significance of conformity signals by comparing with our set of 100 mock catalogues that contain no intrinsic conformity, but do contain the same types of systematic errors that affect the SDSS analysis.

Figure 4 presents our main results of probing 2-halo conformity using quenched fraction differences. The three columns show results for $(g-r)$ colour (left column), sSFR (middle column), and Sérsic index (right column), as measured in the Mr19-SDSS sample and mock catalogues. Each row corresponds to a bin of M_{group} , as listed in the left column of plots. We focus on the four lowest-mass bins since K13 found 2-halo conformity signals at these masses. The black lines in the top portions of each panel show the Δf_q as a function of projected separation r_p , while the shaded contours show the 1σ , 2σ , and 3σ ranges of $\Delta f_{q,\text{mock}}$ for the 100 mock catalogues of each galaxy property. The bottom panels show the residuals of each galaxy property with respect to the mock catalogues, as defined in equation (9).

Figure 4 does not reveal any 2-halo conformity signals for most group masses and scales for $(g-r)$ colour and sSFR. Sérsic index exhibits a prominent 2-halo conformity signal for the two lowest-mass bins, i.e., for group masses of $\log M_{\text{group}} = 11.6\text{--}12.4$ and at scales of $r_p > 3 h^{-1}\text{Mpc}$. This large Sérsic index signal is caused by the fact that SDSS central galaxies in groups of $\log M_{\text{group}} = 11.6\text{--}12.4$ exhibit a small $\Delta f_{\text{early}} = 1\text{--}2\%$ that is constant with scale, while the scatter among the mock catalogues reduces with scale, resulting in a strongly increasing significance of the conformity signal. This figure also shows that the mock results are perfectly centred at $\Delta f_q = 0$, which means that group errors do not seem to impact 2-halo conformity measurements nearly as much as they did in the 1-halo case.

3.2.2 $\mathcal{M}(r_p)$ for 2-halo Conformity

We next study 2-halo conformity using the marked correlation function $\mathcal{M}(r_p)$. We perform a similar analysis as the 1-halo case presented in §3.1.2, except that now we only consider pairs of central galaxies from different groups of similar mass. As with the quenched fraction difference case, we count all central-central pairs with a line-of-sight separation less than $\pi_{\text{max}} = 20 h^{-1}\text{Mpc}$ and place them in logarithmic bins of projected distance r_p . We then compute $\mathcal{M}(r_p)$ for our three galaxy properties after normalizing them by their mean values within M_{group} bins.

To assess the statistical significance of our results and investigate the impact of grouping errors and mass assignment, we compare our SDSS results with measurements on our 100 mock catalogues that contain no built-in 2-halo conformity. Once again, we use the standard deviation of mock $\mathcal{M}(r_p)$ values to estimate the 1σ , 2σ , and 3σ ranges of the mock distribution. We then calculate the residuals of the SDSS measurements with respect to mocks as in equation (10).

Figure 5 shows the $\mathcal{M}(r_p)$ of $(g-r)$ colour (left), sSFR (middle), and Sérsic index (right), as a function of projected

distance, r_p , with each row corresponding to a bin of M_{group} . They layout is similar to that in the previous figures. The figure reveals weak, but highly significant 2-halo conformity signals for all three properties in low mass haloes. In the lowest mass bin, $\log M_{\text{group}} = 11.6\text{--}12.0$, these signals reach a significance as high as 7σ . In the case of $(g-r)$ colour, the signal reaches as high as $\mathcal{M}(r_p) = 1.02\text{--}1.03$ and then declines with scale, while the statistical significance peaks at scales $r_p : 0.6\text{--}4 h^{-1}\text{Mpc}$ and hovers at the 3σ level out to $r_p \sim 10 h^{-1}\text{Mpc}$ before dropping at larger scales. There is no significant large-scale conformity signal in more massive group bins. sSFR behaves the same way, except that the conformity signal is much weaker (yet equally significant), peaking at $\mathcal{M}(r_p)$ value of less than 1.007. In the case of Sérsic index, the signal is also as high as $\mathcal{M}(r_p) = 1.02\text{--}1.03$, but, unlike with colour, it keeps this constant amplitude out to the largest scales we consider. As a result, the statistical significance of the conformity signal keeps rising with scale because the scatter in the mock distribution decreases with scale. In the next mass bin, $\log M_{\text{group}} = 12.0\text{--}12.4$, the conformity signals almost disappear, but are still significant for Sérsic index. There are no 2-halo conformity signals in the higher group mass bins.

These results are similar to what we found using the quenched fraction difference statistic, where Sérsic index displayed the strongest 2-halo conformity signal but only for the low mass groups. However, the marked correlation function is a more sensitive statistic for detecting 2-halo conformity as demonstrated by the much higher statistical significance of the weak observed signals in the case of color and sSFR. Where we found no strong evidence of 2-halo conformity using Δf in Figure 4, we find strong such evidence using $\mathcal{M}(r_p)$ in Figure 5. The marked correlation function is clearly a more sensitive probe of 2-halo conformity than quenched fractions, and gives us a better handle on 2-halo conformity signals for colour and sSFR. In summary, we have found low amplitude, but highly significant 2-halo conformity signals for $(g-r)$ colour and sSFR out to $4 h^{-1}\text{Mpc}$ and an intriguing signal in Sérsic index out to the largest scales that we probe.

4 SUMMARY AND DISCUSSION

In this paper, we study galactic conformity, which is the phenomenon that galaxy properties, such as colour or morphology, may exhibit correlations across distance, beyond what would be expected if these properties only depended on halo mass. At small scales, this “1-halo conformity” is seen as a correlation between the properties of satellite galaxies with those of the central galaxy whose halo they inhabit. At large scales, “2-halo conformity” is seen as a correlation between central galaxies in haloes that are well separated from each other. In both cases, it is important to control for halo mass in order to ensure that any detected correlations are not simply due to the well-established correlations between galaxy properties and halo mass, as well as the correlation between halo mass and larger-scale environment. We are motivated to perform a comprehensive study of conformity because recent works have exposed systematic problems with previous claims of conformity detection at $z = 0$, calling into question whether conformity has actually been detected. In the 1-halo regime, the original detection came from W06 using

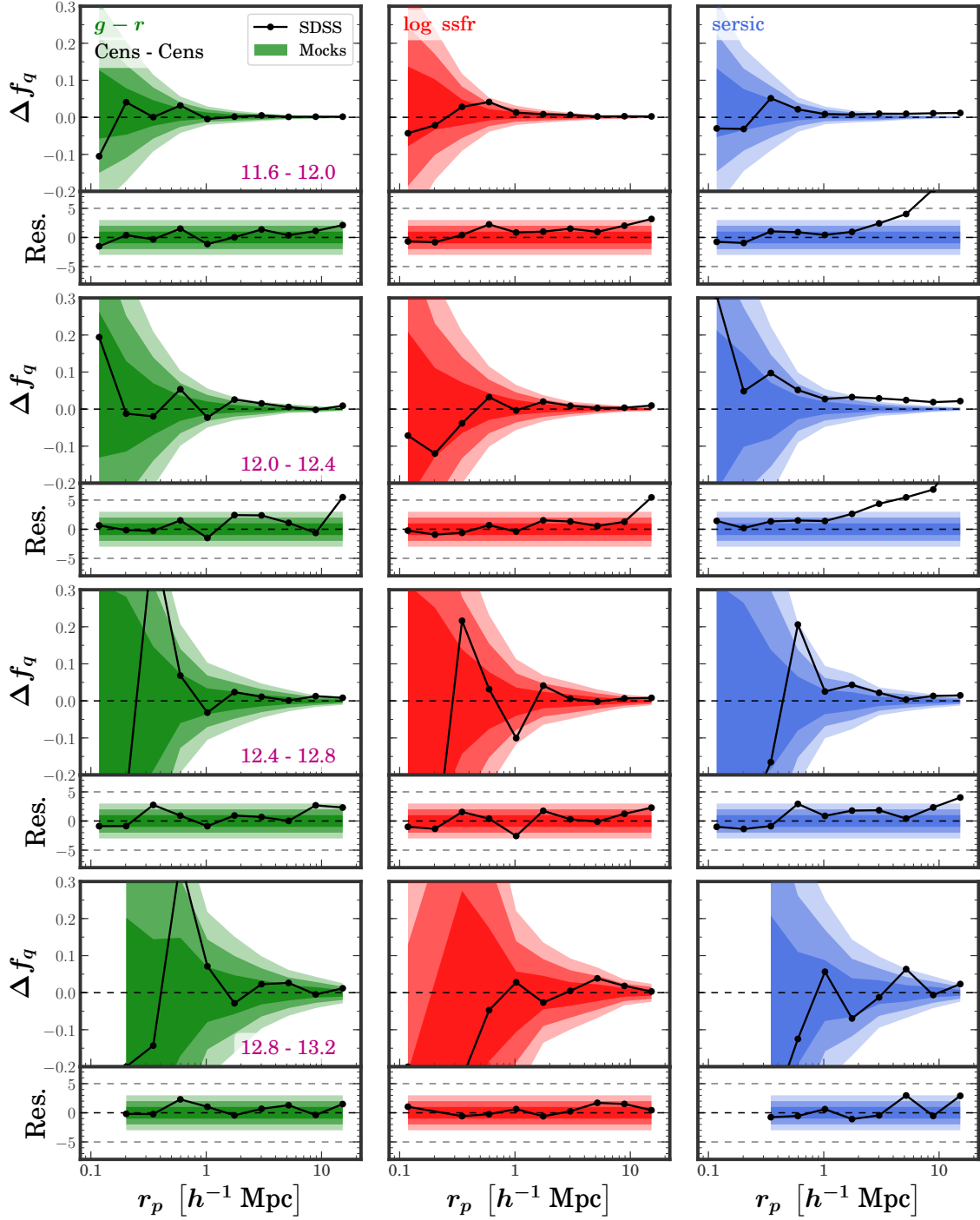


Figure 4. Difference of fractions, Δf , of red (left), passive (centre), and early-type (right) secondary central galaxies as a function of their projected distance, r_p , from primary central galaxies in groups of similar mass, where the difference is measured between primary galaxies that are red and blue, passive and active, early-type and late-type, respectively. Each row corresponds to a bin of group mass, M_{group} , as listed in the left panels. *Top panels:* The solid black lines correspond to the Δf of each galaxy property in Mr19-SDSS. The shaded contours show the 1σ , 2σ , and 3σ ranges of Δf calculated from 100 mock catalogues with no built-in conformity. *Bottom panels:* Normalised residuals of Δf with respect to the mock catalogues. The solid black lines show the difference between Δf for Mr19-SDSS and the mean of the mocks, divided by the standard deviation of Δf for the mocks. The shaded contours show the 1σ , 2σ , and 3σ ranges of the mocks in this normalised space.

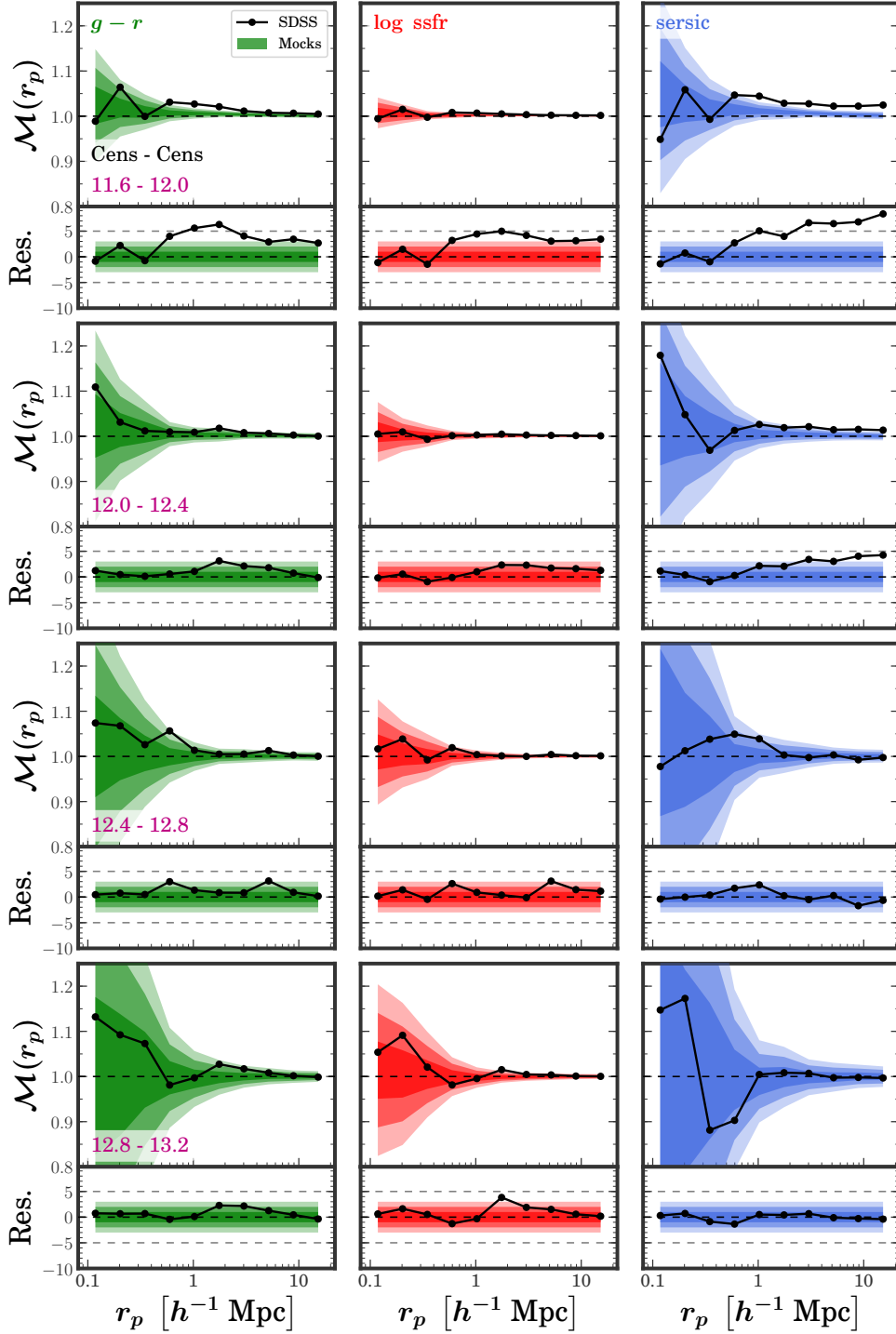


Figure 5. Mark correlation function, $\mathcal{M}(r_p)$, of $(g-r)$ colour (left), sSFR (centre), and Sérsic index (right), as a function of projected distance r_p for central-central galaxy pairs within separate galaxy groups in the Mr19-SDSS sample and mock catalogues. Each row corresponds to a bin of group mass, M_{group} , as listed in the left panels. *Top panels:* The solid black lines show results for SDSS, while the shaded contours show the 1σ , 2σ , and 3σ ranges of $\mathcal{M}(r_p)$ calculated from 100 mock catalogues with no built in 2-halo conformity. *Bottom panels:* Normalised residuals of $\mathcal{M}(r_p)$ with respect to the mock catalogues. The solid black lines show the difference between $\mathcal{M}(r_p)$ of the SDSS and the mean of the mocks, divided by the standard deviation of $\mathcal{M}(r_p)$ for the mocks. The shaded contours show the 1σ , 2σ , and 3σ ranges of the mocks in this normalised space.

a group catalogue to designate central and satellite galaxies and to control for halo mass. However, Campbell (2015) used a mock catalogue to show that errors in group-finding and group mass assignment can lead to a spurious 1-halo conformity signal when none is actually present. In the 2-halo regime, K13 detected conformity out to 4 Mpc using isolation criteria to avoid including satellite galaxies. However, T17 and S17 showed that this result was most likely due to insufficiently stringent isolation criteria and that the detected conformity signal arose from a small number of satellite galaxies that were misidentified as centrals.

We investigate both 1-halo and 2-halo conformity using a galaxy group catalogue from the SDSS DR7. Our analysis contains three main improvements over previous works. First, we study three observed properties of galaxies: $(g-r)$ colour, sSFR, and Sérsic index. Second, we use a new statistic, the marked correlation function, $\mathcal{M}(r_p)$, in addition to the previously used quenched fractions. $\mathcal{M}(r_p)$ is ideally suited for conformity studies and is a more sensitive probe of weak conformity signals. Third, we use a suite of 100 mock galaxy catalogues to quantify the statistical significance of our results. These mock catalogues have the same clustering and same distributions of “observed” properties as the SDSS data (luminosity, $(g-r)$ colour, sSFR, and Sérsic index), and we analyse them in exactly the same way (i.e., same group-finding algorithm, same way of assigning group masses, etc). The mock catalogues do not have any built-in conformity, but they are affected by the same systematic errors as the SDSS data. By comparing our SDSS measurements to the distribution of mock measurements, we can quantify the probability that whatever signal we detect could have arisen from a model with no conformity.

The main results of our work are as follows.

- When measuring the difference between quenched fractions of satellite galaxies around quenched vs. non-quenched centrals, we detect a strong 1-halo conformity signal at all group masses, which is strongest for $(g-r)$ colour, somewhat weaker for sSFR, and only significant at low masses for Sérsic index. These results are in perfect agreement with the results of W06. However, when we compare the $(g-r)$ colour, sSFR, and Sérsic index results to measurements made on our mock catalogues, we find that they are also in perfect agreement. Since the mock catalogues contain no built-in conformity, this strongly suggests that the conformity signal we detected is a result of systematic errors in the group mass estimation and in central/satellite mis-assignment. This calls into question the validity of the W06 detection, as well as other 1-halo conformity detections at $z=0$ that use group catalogues.
- The marked correlation function, $\mathcal{M}(r_p)$, calculated with central-satellite galaxy pairs is sensitive to the radial segregation of satellite galaxy properties within groups. Using the 1-halo $\mathcal{M}(r_p)$, we find significant radial segregation for colour and sSFR at scales smaller than $r_p < 0.2 h^{-1} \text{Mpc}$ in the case of groups more massive than $\log M_{\text{group}} > 13$. We do not find such a signal for Sérsic index. We thus claim a detection of radial segregation in $(g-r)$ color and sSFR.
- After removing the effect of radial segregation from $\mathcal{M}(r_p)$ by properly renormalising galaxy properties, the amplitude of $\mathcal{M}(r_p)$ reduces and the conformity signal mostly vanishes. We thus do not detect 1-halo conformity

using the $\mathcal{M}(r_p)$ statistic in any of the three galaxy properties.

- Studying the quenched fraction difference statistic as a function of projected scale for central-central galaxy pairs in groups of similar mass reveals no 2-halo conformity signal for $(g-r)$ colour or sSFR. However, we find a highly significant 2-halo conformity signal for Sérsic index in low mass groups of $\log M_{\text{group}} < 12.4$. This signal is constant with scale and thus increases in statistical significance with scale. The mock measurements of the three galaxy properties indicate that group errors do not strongly affect our 2-halo quenched fractions, and that the detection of 2-halo conformity in Sérsic index is likely robust.
- The $\mathcal{M}(r_p)$ of central-central galaxy pairs proves to be a more sensitive probe of conformity than quenched fractions. We find a low amplitude, yet highly significant signal in all three galaxy properties for group masses below $\log M_{\text{group}} = 12$. For $(g-r)$ colour and sSFR, the signal is strongest at scales of $r_p : 0.6 - 4 h^{-1} \text{Mpc}$ and hovers at the 3σ level out to $r_p \sim 10 h^{-1} \text{Mpc}$ before dropping at larger scales. For Sérsic index, the 2-halo conformity signal increases in significance with scale. There is no significant large-scale conformity signal in more massive groups. Our detection is unlikely caused by group errors and thus represents robust 2-halo conformity detections in colour, sSFR, and Sérsic index for central-central galaxy pairs at low masses.

These results demonstrate the importance of using mock galaxy catalogues in any study of galactic conformity. Comparing our SDSS measurements with the distribution of mock measurements allows us to test the null model (i.e., no conformity) in a way that includes systematic errors in group-finding or mass estimation. Without the mock catalogues, we would have claimed a strong detection of 1-halo conformity. Instead, we are driven to the conclusion that the 1-halo signal is not real. This result calls into question whether any study has actually detected 1-halo conformity in the SDSS data. The one caveat to these conclusions is that they only hold to the extent that our mock catalogues faithfully represent the real universe. If, for example, the correlation between sSFR and halo mass in the mocks is not as strong as it should be, then the impact of group mass errors on the conformity signal will not be accurate.

In the case of 2-halo conformity, we do not find any statistically significant signals when looking at quenched fractions using colour or sSFR. We thus agree with the claim in T17, that the K13 result must have suffered from errors in the isolation criteria used. On the other hand, we show that the marked correlation function is more sensitive to the underlying weak signal and displays a clear conformity trend, even when compared against the mock catalogues. This measurement may thus represent the first robust detection of 2-halo conformity to-date. Our finding that 2-halo conformity is strongest when considering galaxy Sérsic index is curious and merits further study. Overall, to understand the physical origin of these conformity signals, it will be necessary to model them in detail, which we leave for future work.

5 ACKNOWLEDGEMENTS

The mock catalogues used in this paper were produced by the LasDamas project (<http://lss.phy.vanderbilt.edu/lasdamas/>); we thank NSF XSEDE for providing the computational resources for LasDamas. Some of the computational facilities used in this project were provided by the Vanderbilt Advanced Computing Center for Research and Education (ACCRE). This project has been supported by the National Science Foundation (NSF) through a Career Award (AST-1151650). Parts of this research were conducted by the Australian Research Council Centre of Excellence for All Sky Astrophysics in 3 Dimensions (ASTRO 3D), through project number CE170100013. This research has made use of NASA's Astrophysics Data System. This work made use of the IPython package (Pérez & Granger 2007), Scikit-learn (McKinney 2010), SciPy (Jones 2001), matplotlib, a Python library for publication quality graphics (Hunter 2007), Astropy, a community-developed core Python package for Astronomy (Astropy Collaboration et al. 2013), and NumPy (Van Der Walt et al. 2011). Funding for the SDSS and SDSS-II has been provided by the Alfred P. Sloan Foundation, the Participating Institutions, the National Science Foundation, the U.S. Department of Energy, the National Aeronautics and Space Administration, the Japanese Monbukagakusho, the Max Planck Society, and the Higher Education Funding Council for England. The SDSS Web Site is <http://www.sdss.org/>. The SDSS is managed by the Astrophysical Research Consortium for the Participating Institutions. The Participating Institutions are the American Museum of Natural History, Astrophysical Institute Potsdam, University of Basel, University of Cambridge, Case Western Reserve University, University of Chicago, Drexel University, Fermilab, the Institute for Advanced Study, the Japan Participation Group, Johns Hopkins University, the Joint Institute for Nuclear Astrophysics, the Kavli Institute for Particle Astrophysics and Cosmology, the Korean Scientist Group, the Chinese Academy of Sciences (LAMOST), Los Alamos National Laboratory, the Max-Planck-Institute for Astronomy (MPIA), the Max-Planck-Institute for Astrophysics (MPA), New Mexico State University, Ohio State University, University of Pittsburgh, University of Portsmouth, Princeton University, the United States Naval Observatory, and the University of Washington. These acknowledgements were compiled using the Astronomy Acknowledgement Generator.

References

- Abazajian K., et al., 2004, *The Astronomical Journal*, 128, 502
- Abazajian K. N., et al., 2009, *The Astrophysical Journal Supplement Series*, 182, 543
- Adelman-McCarthy J. K., et al., 2007, *The Astrophysical Journal Supplement Series*, 172, 634
- Aihara H., et al., 2011, *The Astrophysical Journal Supplement Series*, 193, 29
- Ann H. B., Park C., Choi Y. Y., 2008, *Monthly Notices of the Royal Astronomical Society*, 389, 86
- Astropy Collaboration et al., 2013, *\aap*, 558, A33
- Beisbart C., Kerscher M., 2000, *The Astrophysical Journal*, 545, 6
- Berlind A. A., Weinberg D. H., 2002, *The Astrophysical Journal*, 575, 587
- Berlind A. a., et al., 2006, *The Astrophysical Journal Supplement Series*, 167, 1
- Berti A. M., Coil A. L., Behroozi P. S., Eisenstein D. J., Bray A. D., Cool R. J., Moustakas J., 2017, *The Astrophysical Journal*, 834, 87
- Blanton M. R., et al., 2003, *The Astrophysical Journal*, 592, 819
- Blanton M. R., et al., 2005, *The Astronomical Journal*, 129, 2562
- Bray A. D., et al., 2016, *Monthly Notices of the Royal Astronomical Society*, 455, 185
- Brinchmann J., Charlot S., White S. D. M., Tremonti C., Kauffmann G., Heckman T., Brinkmann J., 2004, *Monthly Notices of the Royal Astronomical Society*, 351, 1151
- Cacciato M., Van Den Bosch F. C., More S., Li R., Mo H. J., Yang X., 2009, *Monthly Notices of the Royal Astronomical Society*, 394, 929
- Campbell L. E., 2015, PhD thesis, The Vanderbilt University, <http://etd.library.vanderbilt.edu/available/etd-03192015-152945/>
- Campbell D., van den Bosch F. C., Hearin A., Padmanabhan N., Berlind A., Mo H. J., Tinker J., Yang X., 2015, *Monthly Notices of the Royal Astronomical Society*, 452, 444
- Coil A. L., et al., 2011, *The Astrophysical Journal*, 741, 8
- Cool R. J., et al., 2013, *The Astrophysical Journal*, 767, 118
- Croton D. J., Gao L., White S. D. M., 2007, *Monthly Notices of the Royal Astronomical Society*, 374, 1303
- Davis M., Efstathiou G., Frenk C. S. S., White S. D. M. D. M., 1985, *The Astrophysical Journal*, 292, 371
- Doi M., et al., 2010, *The Astronomical Journal*, 139, 1628
- Gao L., Springel V., White S. D. M., 2005, *Monthly Notices of the Royal Astronomical Society: Letters*, 363, L66
- Gunn J. E., et al., 1998, *The Astronomical Journal*, 116, 3040
- Gunn J. E., et al., 2006, *The Astronomical Journal*, 131, 2332
- Guo Q., et al., 2011, *Monthly Notices of the Royal Astronomical Society*, 413, 101
- Hartley W. G., Conselice C. J., Mortlock A., Foucaud S., Simpson C., 2015, *Monthly Notices of the Royal Astronomical Society*, 451, 1613
- Hearin A. P., Watson D. F., van den Bosch F. C., 2015, *Monthly Notices of the Royal Astronomical Society*, 452, 1958
- Hearin A. P., Behroozi P. S., van den Bosch F. C., 2016, *Monthly Notices of the Royal Astronomical Society*, 461, 2135
- Huchra J. P., Geller M. J., 1982, *The Astrophysical Journal*, 257, 423
- Hunter J. D., 2007, *Computing In Science & Engineering*, 9, 90
- Kauffmann G., et al., 2003, *Monthly Notices of the Royal Astronomical Society*, 341, 33
- Kauffmann G., Li C., Heckman T. M., 2010, *Monthly Notices of the Royal Astronomical Society*, 409, 491
- Kauffmann G., Li C., Zhang W., Weinmann S., 2013, *Monthly Notices of the Royal Astronomical Society*, 430, 1447
- Kawinwanichakij L., et al., 2016, *The Astrophysical Journal*, 817, 9
- Knobel C., Lilly S. J., Woo J., Kovač K., 2015, *The Astrophysical Journal*, 800, 24
- Lacerna I., Contreras S., González R. E., Padilla N., Gonzalez-Perez V., 2018, *Monthly Notices of the Royal Astronomical Society*, 475, 1177
- Lawrence A., et al., 2007, *Monthly Notices of the Royal Astronomical Society*, 379, 1599
- Martinez V. J., Arnalte-Mur P., Stoyan D., 2010, <http://arxiv.org/abs/1001.1294>, 22, 6
- McBride C., Berlind A., Scoccimarro R., Wechsler R., Busha M., Gardner J., van den Bosch F., 2009, *American Astronomical Society Meeting Abstracts #213*, 41, 425.06
- McCracken H. J., et al., 2012, *Astronomy & Astrophysics*, 544, A156
- McKinney W., 2010, in van der Walt S., Millman J., eds, *Proceedings of the 9th Python in Science Conference*. pp 51–56

- Paranjape A., Kovač K., Hartley W. G., Pahwa I., 2015, *Monthly Notices of the Royal Astronomical Society*, 454, 3030
- Pérez F., Granger B. E., 2007, *Computing in Science and Engineering*, 9, 21
- Phillips J. I., Wheeler C., Boylan-Kolchin M., Bullock J. S., Cooper M. C., Tollerud E. J., 2014a, *Monthly Notices of the Royal Astronomical Society*, 437, 1930
- Phillips J. I., Wheeler C., Cooper M. C., Boylan-Kolchin M., Bullock J. S., Tollerud E., 2014b, *Monthly Notices of the Royal Astronomical Society*, 447, 698
- Prescott M., et al., 2011, *Monthly Notices of the Royal Astronomical Society*, 417, 1374
- Ross A. J., Brunner R. J., 2009, *Monthly Notices of the Royal Astronomical Society*, 399, 878
- Salcedo A. N., Maller A. H., Berlind A. A., Sinha M., McBride C. K., Behroozi P. S., Wechsler R. H., Weinberg D. H., 2017, eprint arXiv:1708.08451
- Salim S., et al., 2007, *The Astrophysical Journal Supplement Series*, 173, 267
- Sheth R. K., Connolly A. J., Skibba R., 2005, 13, 13
- Sin L. P. T., Lilly S. J., Henriques B. M. B., 2017, *Monthly Notices of the Royal Astronomical Society*, 471, 1192
- Skibba R., Sheth R. K., Connolly A. J., Scranton R., 2006, *Monthly Notices of the Royal Astronomical Society*, 369, 68
- Smee S. A., et al., 2013, *The Astronomical Journal*, 146, 32
- Tinker J. L., Hahn C., Mao Y.-Y., Wetzel A. R., Conroy C., 2018, *Monthly Notices of the Royal Astronomical Society*, 477, 935
- Van Den Bosch F. C., Yang X., Mo H. J., 2003, *Monthly Notices of the Royal Astronomical Society*, 340, 771
- Van Der Walt S., Colbert S. C., Varoquaux G., 2011, *Computing in Science & Engineering*, 13, 22
- Vogelsberger M., et al., 2014, *Monthly Notices of the Royal Astronomical Society*, 444, 1518
- Wang W., White S. D. M., 2012, *Monthly Notices of the Royal Astronomical Society*, 424, 2574
- Wang J., et al., 2015, *Monthly Notices of the Royal Astronomical Society*, 453, 2400
- Warren M. S., Abazajian K., Holz D. E., Teodoro L., 2006, *The Astrophysical Journal*, 646, 881
- Wechsler R. H., Zentner A. R., Bullock J. S., Kravtsov A. V., Allgood B., 2006, *The Astrophysical Journal*, 652, 71
- Weinmann S. M., Van Den Bosch F. C., Yang X., Mo H. J., 2006, *Monthly Notices of the Royal Astronomical Society*, 366, 2
- Yang X., Mo H. J., Van den Bosch F. C., 2003, *Monthly Notices of the Royal Astronomical Society*, 339, 1057
- Yang X., Mo H. J., Van Den Bosch F. C., Jing Y. P., 2005, *Monthly Notices of the Royal Astronomical Society*, 356, 1293
- Yang X., Mo H. J., Bosch F. C. V. D., Pasquali A., Li C., Barden M., 2007, *The Astrophysical Journal*, 671, 153
- Yang X., Mo H. J., Bosch F. C. v. d., Zhang Y., Han J., 2012, *The Astrophysical Journal*, 752, 41
- York D. G., et al., 2000, *The Astronomical Journal*, 120, 1579
- Zehavi I., et al., 2005, *The Astrophysical Journal*, 630, 1
- Zehavi I., et al., 2010, *The Astrophysical Journal*, 59, 35
- Zu Y., Mandelbaum R., 2015, *Monthly Notices of the Royal Astronomical Society*, 454, 1161
- Zu Y., Mandelbaum R., 2016, *Monthly Notices of the Royal Astronomical Society*, 457, 4360
- Zu Y., Mandelbaum R., 2018, *Monthly Notices of the Royal Astronomical Society*, 476, 1637
- 2001, {SciPy}: Open source scientific tools for Python, <http://www.scipy.org/>

This paper has been typeset from a \LaTeX file prepared by the author.